JOURNAL OF MATERIALS SCIENCE **36** (2001) 593–601

Modelling primary recrystallization and grain growth in a low nickel austenitic stainless steel

A. DI SCHINO, J. M. KENNY
Materials Engineering Center, University of Perugia, TERNI, Italy
E-mail: Kenny@unipg.it

I. SALVATORI, G. ABBRUZZESE
Centro Sviluppo Materiali, Italy

This paper deals with the recrystallization and grain growth processes of a low nickel stainless steel. Samples of steel sheets with various cold rolling degrees were annealed at different temperatures and the recrystallization and grain growth kinetics have been studied. The grain size of the samples has been determined via automatic image analysis and transformed to 3-D values according to the Saltykov model. The experimental data have been analysed according to a modified model developed using the statistical approach by Abbruzzese and Lucke for the grain growth. This approach supplies a unified equation describing at the same time primary recrystallization and grain growth. The values of the dislocation density obtained from the comparison of theoretical predictions and experimental data of the grain mean radius are properly correlated to the mechanical properties of the steel.

1. Introduction

Nickel containing austenitic stainless steels have been indispensable for the progress of technology during the last 80 years. Due to the cost of nickel and to the prospected possibility of allergic reactions caused by this element, more and more laboratories and industries are trying to develop a new class of austenitic stainless steels without nickel [1–4].

To maintain the austenitic microstructure, Ni reduction is balanced by nitrogen addition. These nitrogen alloyed austenitic stainless steels exhibit attractive properties as high strength and ductility, good corrosion resistance and reduced tendency to grain boundary sensitation [5]. Since nitrogen increases the stability of austenite phase against the martensite formation [6], nitrogen alloyed austenitic stainless steels can be strengthened by cold working without any massive formation of strain induced martensite, leading to higher mechanical properties and to a good balance between toughness and tensile properties. In this new class of stainless steels the presence of a high manganese content is required to attain the high nitrogen concentration in the melt avoiding the tendency to Cr_2N formation [7].

A deep understanding of the recrystallization and grain growth processes is needed as they reflect on the mechanical properties of the steel. Nonetheless, these mechanisms have not been investigated in low nickel austenitic stainless steels. Then, the primary recrystallization and grain growth in a low nickel austenitic stainless steel are here studied using a statistical model.

2. Outline of the statistical model

It is well known that the driving force of primary recrystallization is mainly related to the system tendency to eliminate the deformation energy (dislocations) introduced by cold working. The release of the deformation energy during heat treatment, activates the movement of dislocations and subgrain boundaries thus restoring a "dislocation free" microstructure. Under further heat treatment grain growth, activated by boundary energy reduction, is the predominant process.

There have been several attempts to simulate primary recrystallization by computer modelling [8–10]. Such models are capable of predicting grain size distributions as well recrystallization kinetics. Several theories have also been developed to simulate the behaviour of grain growth after primary recrystallization. These theories do not describe the behaviour of single grains, and allow only statistical averages of the behaviour to be derived. Early theories were due to Hillert [11] and to Cahn and Pedawar [12].

Although the large number of existing models, they are not sophisticated enough to treat simultaneously and continuously both recrystallization and grain growth. In the study reported here, an integrated mathematical model, able to describe the primary recrystallization and grain growth in low nickel austenitic stainless steel as interplaying phenomena is used.

In this preliminary application, the model assumes the case of "uniform grain boundary", namely it does not take into account any orientation differences between the different grains. Although at the present the theoretical foundations of the statistical model has been

recognised to be strictly linked to fundamental laws [13, 14], here, for the sake of simplicity, a more heuristic approach is used [15–17]. The model is based on three further assumptions:

The assumption of superposition of average grain curvatures in individual grain boundaries. A grain ν characterised by a volume V_ν is assumed to grow at the expenses of a neighbouring grain μ with a rate:

$$\left(\frac{\mathrm{d}V_\nu}{\mathrm{d}t}\right)_\mu = s_{\nu\mu} m 2\gamma \left(\frac{1}{R_\mu} - \frac{1}{R_\nu}\right) = M s_{\mu\nu}\left(\frac{1}{R_\mu} - \frac{1}{R_\nu}\right) \quad (1)$$

where R_ν is the radius of a grain ν, $s_{\nu\mu}$ $(=s_{\mu\nu})$ is the area of contact between the two grains ν and μ, and m, γ, and $M = 2m\gamma$ represent the mobility, the surface tension and the grain boundary $(\mu\nu)$ diffusivity respectively.

By taking into accounts all N_ν neighbours of a grain the total growth rate is obtained:

$$\left(\frac{\mathrm{d}R_\nu}{\mathrm{d}t}\right) = \frac{1}{4\pi R_\nu^2}\frac{\mathrm{d}V_\nu}{\mathrm{d}t} = \frac{1}{4\pi R_\nu^2} M \sum_{\mu=1}^{N_\nu} s_{\mu\nu}\left(\frac{1}{R_\mu} - \frac{1}{R_\nu}\right) \quad (2)$$

with $\mu = 1, 2, \ldots, N_\mathrm{G}$ and N_G being the total number of grains in the unit volume. This expression represents a system of N_G differential equations for the unknowns $R_\nu(t)$. Due to the large number of grains N_G, and thus of differential equations necessary to obtain a significant simulation, this leads to great computational difficulties. Therefore, further simplifying assumptions are introduced in the model.

The assumption of homogeneous surroundings of the grains. As a first approximation it is assumed that a surrounding matrix, identical for all the grains with the same radius, can replace the individual neighbourhood of any grain. Following this assumption all the grains of the same size will grow with the same rate. Then, they can be collected in classes characterised by their size R_i and frequency n_i and the analysis can be scaled up to study the behaviour a grain classes, instead of single grains.

From the mathematical point of view the simplification consists in replacing in Equation 1 the individual contact areas $s_{\mu\nu}$ by averaged areas a_{ij}, where $a_{ij} = \frac{A_{ij}}{n_i}$, n_j is the total number of grains in class j and A_{ij} is the total area of contact between the two classes i and j. Then, it follows that:

$$\frac{\mathrm{d}R_i}{\mathrm{d}t} = \frac{M}{4\pi R_i^2}\sum_j a_{ij}\left(\frac{1}{R_j} - \frac{1}{R_i}\right) \quad (4)$$

The assumption of a random array of the grains, namely the probability of contact among the grains is only depending on their relative surface in the system. In this case the area of a grain of the class i is divided between the neighbouring grains of the class j in proportion to the individual surface area:

$$a_{ij} = 4\pi R_i^2 p_j, \quad p_j = \frac{n_j R_j^2}{\sum_j n_j R_j^2} \quad (5)$$

The integration of all the above assumptions in the model leads to the following final form of the grain growth rate equation:

$$\frac{\mathrm{d}R_i}{\mathrm{d}t} = M\sum_j\left(\frac{1}{R_j} - \frac{1}{R_i}\right)p_j \quad (6)$$

To describe the recrystallization process integrated with the grain growth, it is necessary to propose an extended growth equation which enables to contemporarily and continuously analyse the evolution of free nuclei in the matrix passing through partially impinged grains up to full contact.

For recrystallization a nucleus must have the following characteristics:

- It must be more perfect than its neighbours; that is, it must contain fewer dislocations and thereby a lower strain energy.
- The boundaries of the subgrain must be mobile by virtue of sufficient lattice misorientation between the subgrain and its neighbours. Sufficient misorientation might be about 15°, referred to a common axis of rotation.
- It must be large enough so that the additional interfacial energy that must be supplied for growth is less than the volume free energy released when strained cells are replaced by a strain-free subgrain.

In our approach recrystallization nuclei (sub-grains) are considered pre-existing in the deformed microstructure and characterized by their size distribution. Moreover, the grains are assumed to be all activated from the beginning and freely growing in the deformed matrix until they get in contact to each other. This process is characterised by a gradual transition from a deformation gradient activated growth, to a proper grain growth process activated by only boundary energy reduction. The final integrated equation for recrystallization and grain growth can therefore be written as:

$$\frac{\mathrm{d}R_i}{\mathrm{d}t} = m_1\left(\frac{Gb^2}{3}\Delta\rho - \frac{2\gamma_1}{R_i}\right)\sum_{j=1}^{i^*-1} p_j + m_2\gamma_2\sum_{j=i^*}^{n_c} p_j\left(\frac{1}{R_j} - \frac{1}{R_i}\right) \quad (7)$$

where G is the shear modulus of the material, b is the Burger vector, ρ is the dislocation density, $\Delta\rho = \rho_\mathrm{d} - \rho_\mathrm{r}$, is the difference between the dislocation densities in the deformed and in the recrystallized

material; m_1, γ_1, m_2 and γ_2 are the grain boundary mobility and the surface energy of the freely growing grains in the deformed matrix and that of grains in contact respectively; i^* is the minimum class index of grains in contact with grains "i".

Assuming $m_1 \approx m_2$ and $\gamma_1 \approx \gamma_2$ [18], Equation 7 can be written as:

$$\frac{\mathrm{d}R_i}{\mathrm{d}t} = m\left[\left(\frac{Gb^2}{3}\Delta\rho - \frac{2\gamma}{R_i}\right)\sum_{j=1}^{i^*-1} p_j + \gamma\sum_{j=i^*}^{n_c} p_j\left(\frac{1}{R_j} - \frac{1}{R_i}\right)\right] \quad (8)$$

The criterion for identifying the critical class i^*, is obtained by defining an average influence volume, and consequently an influence radius R_m, calculated as follows:

$$V_\mathrm{M} = \frac{1}{N_\mathrm{T}} - \sum_{i=1}^{n}\frac{n_i v_i}{N_\mathrm{T}} = \frac{1}{N_\mathrm{T}}(1 - F_\mathrm{V}) \quad (9)$$

where N_T is the total number of grains per cm^3, F_V is the recrystallized volume fraction and v_i is the volume of the grain of the class and n_i is the number of grains of volume v_i. R_m varies from $(3/4\pi N_\mathrm{T})^{1/3}$ to zero when all the grains are in contact. Then, the R_m parameter defines an index i^* that discriminates the class over which all the grains are in contact.

3. Materials and experimental procedure

The chemical composition of the low nickel steel (hereafter LNi) studied in this paper is shown in Table I. In particular, it can be noted the high content of nitrogen, which favours the γ-phase stability and increases the mechanical properties of the steel, and the high content of manganese, which favours the solubilisation of nitrogen.

Samples of low Ni and high N steel were cold rolled down to different thickness with reduction grades of 80% (1 mm thickness), 60% (2 mm thickness), 40% (3 mm thickness) and then annealed in laboratory at $T = 1100\,^\circ$C for different times (up to 5 min). Temperature-time profiles during heating and quenching were measured and interpolated by polynomial fitting. After electrochemical etching in a solution containing HNO_3 and HCl, samples were analysed for grain size determination through automatic optical image analyser. Micro-hardness measurements were performed on the samples and related to the recrystallized volume fraction. Tensile stresses were related to the dislocation density ρ used as a fitting parameter in the statistical model.

TABLE I Chemical compositions of the material (mass %)

	C	Mn	Ni	Cr	N	Mo	Cu	S	P	Si
LNi	0.026	10.5	0.42	18.6	0.40	0.07	0.07	0.003	0.026	0.04

4. Results and discussion

4.1. Data elaboration

After grain size determination by automatic image analyser, experimental data have been transformed in 3-D according to the Saltykov model [19] and fitted by the statistical recrystallization model.

The temperature dependence of the boundary mobility was taken into account through the incorporation of the measured heating profiles in the microstructural model accordingly with the Stokes-Einstein relationship:

$$m = \frac{D}{K_\mathrm{B}T} = \frac{D_0}{K_\mathrm{B}T}\,e^{-\frac{\Delta E}{K_\mathrm{B}T}} \quad (10)$$

where D is the diffusion coefficient, K_B is the Boltzmann constant, ΔE is the activation energy of the process, T is the temperature. It is thus possible to take into accounts the effect of the annealing treatment on the material, by introducing in Equation 10 the function $T = T(t)$ from the measured temperature-time profile.

D was chosen as a first approximation proportional to the diffusion coefficient of Fe in Fe-γ [20]. The proportional coefficient has been hold constant for all simulations corresponding to the three different cold rolling reduction grades. The value of the proportionality coefficient between the grain boundary mobility in the low nickel steel as obtained by fitting the experimental data, and the one of Fe-γ was 3×10^{-6}. The initial number of nuclei N and the dislocation density ρ, the other input parameters of the model, were considered as dependent of the cold reduction grade. From a sensitivity study of the model parameters, it came out that the shape of the initial grain size distribution and the volume fraction of the nuclei are not very effective on the kinetics whereas the variation of the number of nuclei N is much more effective. Moreover it must be considered that the average size of nuclei is linked with N in such a way that the higher the number of nuclei the lower is their size. Considering the limited effect on the kinetics and on the final results on the distribution of grain radii, it has been assumed that the initial volume fraction and the shape of the size distribution of the nuclei are not function of the degree of deformation. Then, for all reduction grades, the average size of nuclei can be calculated directly from the number N of nuclei.

Moreover a variation coefficient k can be defined as $k = \sigma/R$, where σ is the standard deviation of the radius distribution and R is the mean radius. The parameter k has been widely used to describe and compare grain growth in metals.

4.2. Prediction if the mean radius and of the variation coefficient

The experimental mean radii of samples of cold rolled LNi steel at three different reduction grades (40%, 60%, 80%) and annealed at different times are shown in Figs 1–3. The comparison between the variation coefficient as obtained by the statistical model and by automatic image analyser is also shown. These results

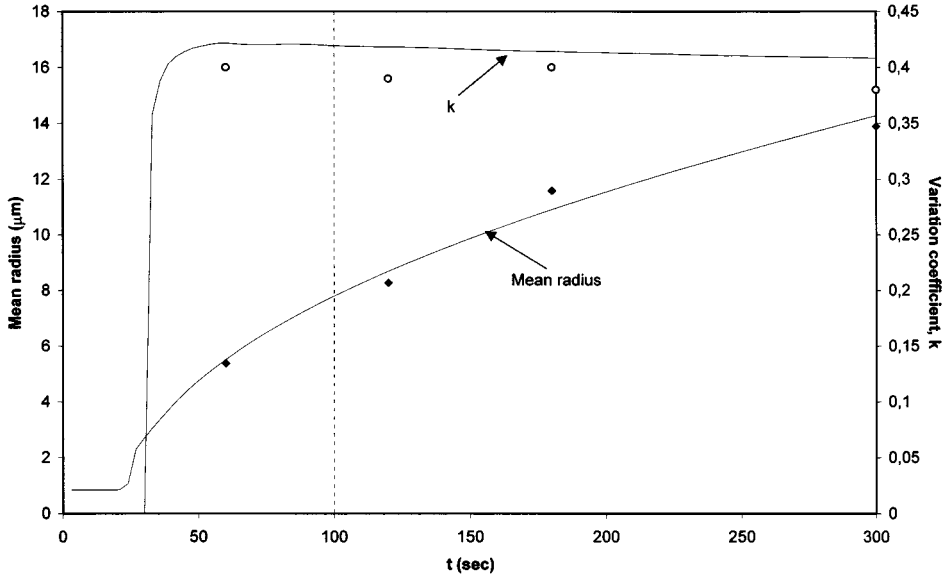

Figure 1 Mean radius and variation coefficient versus time in the 40% sample. The dashed line represents the time at which $T = 1100\,^{\circ}\mathrm{C}$ is reached during the annealing. The continuous lines represent the simulations according to the statistical model.

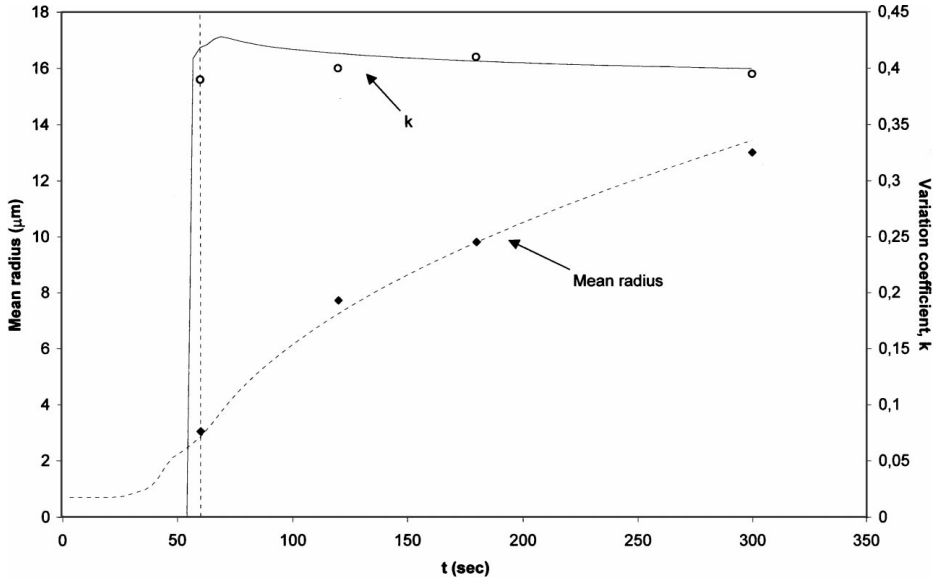

Figure 2 Mean radius and variation coefficient versus time in the 60% sample. The dashed line represents the time at which $T = 1100\,^{\circ}\mathrm{C}$ is reached during the annealing. The continuous lines represent the simulations according to the statistical model.

TABLE II Dislocation density and initial number of nuclei used as input parameters in the simulations

Cold reduction grade	Dislocation density, ρ (cm^{-2})	Initial number of nuclei, N (cm^{-3})
40 %	5.0×10^{9}	8.6×10^{9}
60 %	2.0×10^{10}	1.7×10^{10}
80 %	1.0×10^{11}	3.0×10^{10}

show a good agreement between the prediction of the model and experimental data. The values of the best fitting parameters used for the simulations are shown in Table II.

Although a smaller mean radius with a higher cold reduction should be expected, the same mean radius values have been obtained for all reduction grades. It must be noted that, due to the different thickness of the samples (which come from the same hot rolled coil), the higher is the cold reduction the higher is the subsequent heating rate. Therefore, opposite effects are produced by cold reduction and by the heating rate during grain growth.

In order to better analyse the effects of the heating profile on the mean radius during recrystrallization and grain growth a specific set of simulations has been performed on three LNi strips with different initial thickness (1 mm, 2 mm, 3 mm) cold rolled with the same reduction grade (80%). The results of the simulations (using the microstructural parameters $\rho = 10^{11}$ cm^{-2}, $N = 3{*}10^{10}$ cm^{-3}) are shown in Fig. 4. From these results it is evident that the different heating profiles, due to the thickness effect, influence significantly the grain size showing in particular the relevance of the "time" spent by the sample at the highest temperatures.

The calculated numbers of nuclei and dislocations densities are shown in Fig. 5 as a function of the cold reduction grade. These results not only reflect the expected behaviour of the recrystallization and

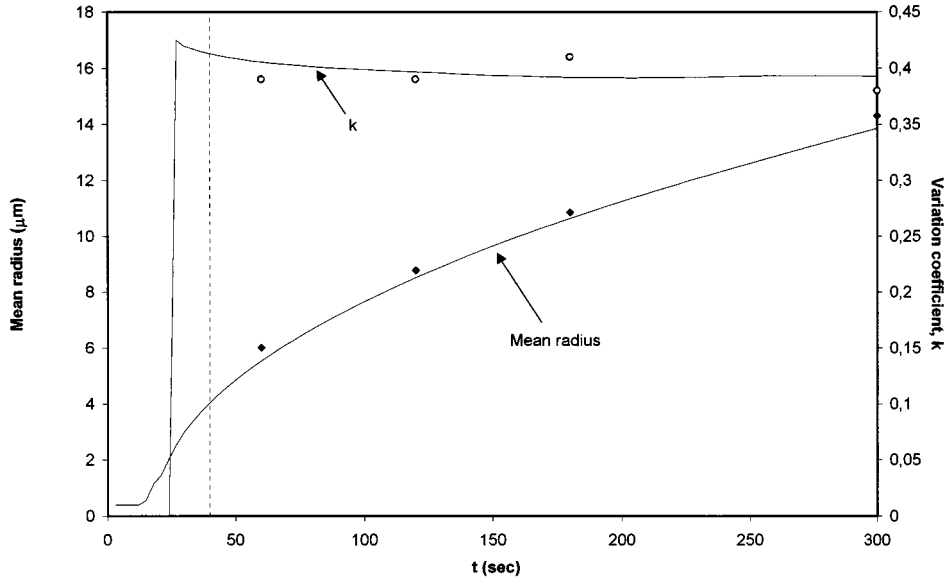

Figure 3 Mean radius and k versus time in the 80% sample. The dashed line represents the time at which $T = 1100\,^{\circ}\mathrm{C}$ is reached during the annealing. The continuous lines represent the simulations according to the statistical model.

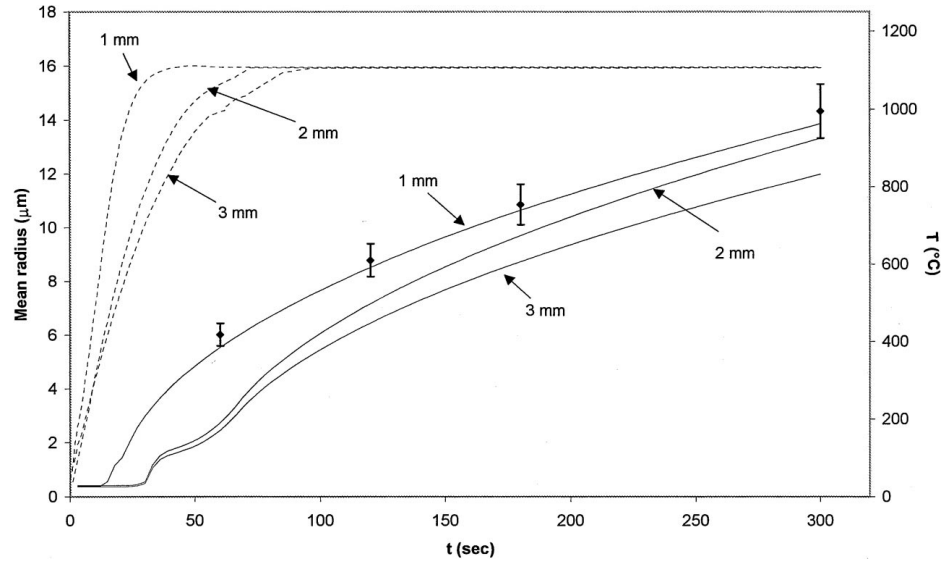

Figure 4 Influence of the heating profile on the mean radius (continuos lines) calculated according to the statistical model ($\rho = 1 * 10^{11}$ cm^{-2}, $N = 3 * 10^{10}$ cm^{-3}, used for 80% cold reduction) and the experimental heating profiles (dashed lines) corresponding to 1 mm, 2 mm, 3 mm.

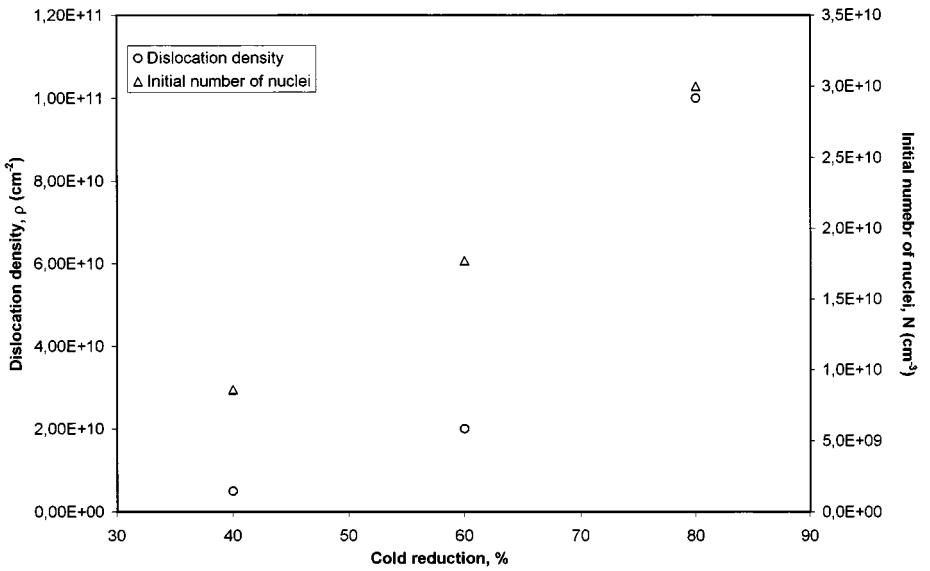

Figure 5 Initial number of nuclei N and dislocations density ρ as a function of the cold reduction.

grain growth process but also represent the connection between the microstructure characteristics of the deformed material and the processing parameters. It is also worth to mention the tendency to saturation of the number of nuclei as a function of the dislocation density shown at high cold reduction grades (see Fig. 6). Figs 5 and 6 are also of practical importance since, once the model has been set for a given steel, it is possible to obtain from them the parameters to simulate the behaviour of the same material subjected to different cold reduction grades.

In order to indirectly validate the dislocation density data inserted in the model as an input parameter, the validity of the Taylor dependency between ρ and the flow stress σ_m, which has been found valid in polycrystalline materials [21], has been tested:

$$\sigma_m \propto \langle \rho \rangle^{0.5} \tag{11}$$

In Equation 11, ρ is the value obtained by best fitting of the experimental mean radius with the statistical model and the σ_m is obtained by tensile stress test. The results of this correlation are shown in Fig. 7 where a good agreement ($n = 0.43$ in comparison to the theoretical $n = 0.5$) between simulation results and Equation 11 results are obtained. This result is an indirect proof that the dislocations density ρ already identified by the model through the best fitting of the mean radius and the variation coefficient values, are congruent with the experimental data σ_m.

4.3. Prediction of the recrystallized volume fraction

Due to the general difficulty in determining the recrystallized fraction by automatic image analyser in partially recrystallized samples, a model has been developed relating the recrystallized fraction to the steel hardness. Because it is well known that the hardness δ is with good approximation proportional to the tensile strength of the steels, from Equation 11 it can be written:

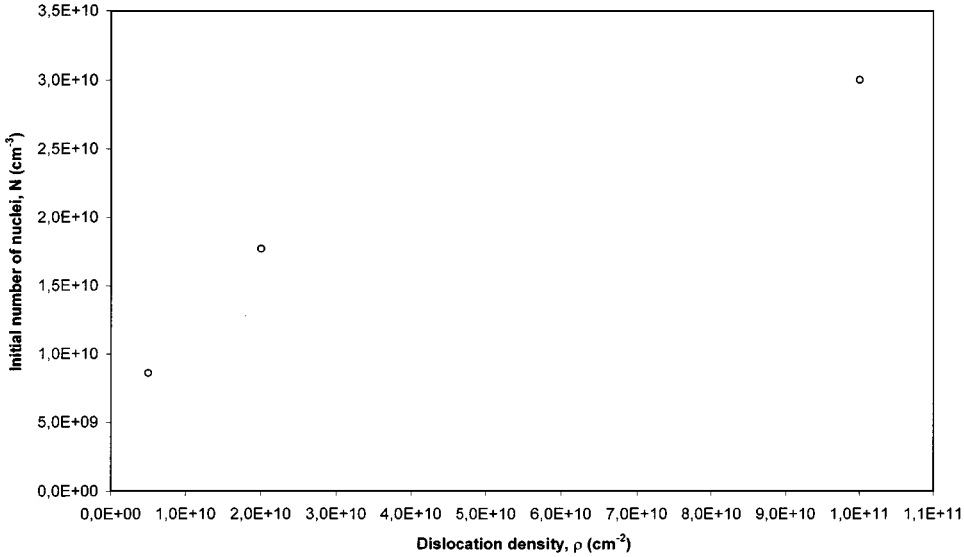

Figure 6 Initial number of nuclei N versus dislocation density ρ.

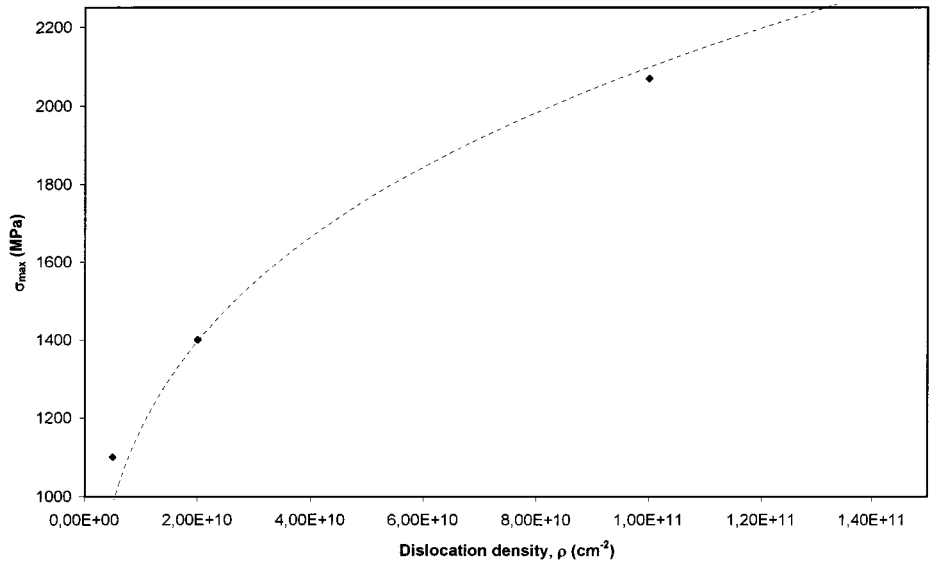

Figure 7 Power relation between experimental tensile stress and dislocation density. The dashed line represents the fitting according to $\sigma_m = k\rho^n$, $n = 0.43$.

$$\delta \propto \sigma_m \propto \sqrt{\langle \rho \rangle} \tag{12}$$

where δ is the average value of the hardness of the steel.

On the other hand, the following relation in terms of dislocation density and recrystallized volume fraction can be written:

$$\langle \rho \rangle = \rho_R F_V + \rho_C (1 - F_V) \tag{13}$$

where $\langle \rho \rangle$ is the mean dislocation density in the steel, ρ_R is the dislocation density of the annealed steel and ρ_C corresponds to the deformed steel before annealing. This relationship is a simple weighted average of the dislocation density specifically when no recovery phenomena occur (as it can be considered with a good approximation for an austenitic matrix) whose presence could complicate Equation 13 making variable ρ_C during the heat treatment depending on a law which should be defined.

From Equations 12 and 13 it follows that:

$$F_V = \alpha + \beta \delta^2 \tag{14}$$

with α and β constant parameters.

From the boundary conditions $\delta(F_V = 0) = \delta_C$ and $\delta(F_V = 1) = \delta_R$ the following relation can be written between the recrystallized fraction and the hardness of the steel as a function of the annealing time t:

$$F_V(t) = \frac{\delta^2(t) - \delta_C^2}{\delta_R^2 - \delta_C^2} \tag{15}$$

The comparison of the values of the recrystallized volume fraction obtained from hardness measurements and those obtained from the statistical model is shown in Figs 8–10 for the three different cold reduction grades.

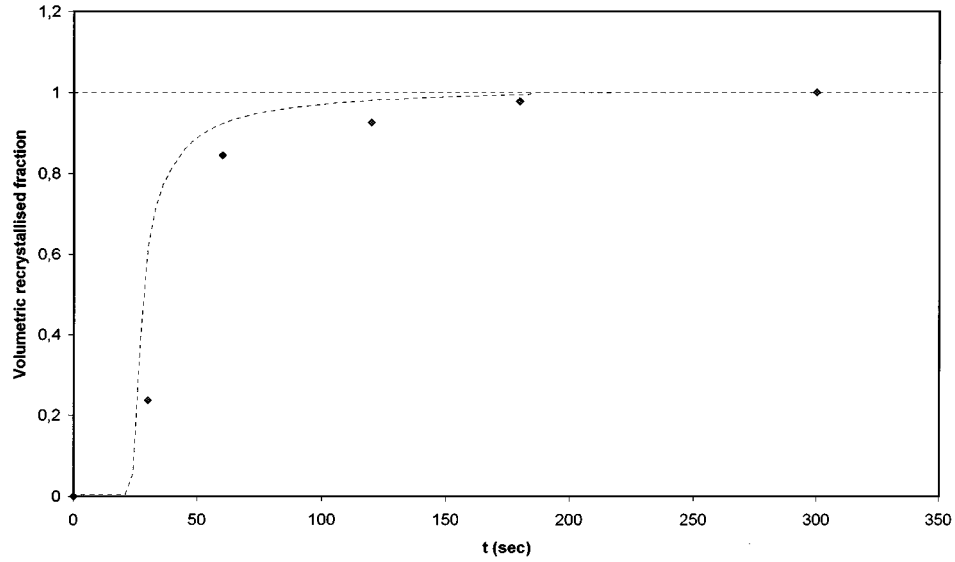

Figure 8 Comparison between the prediction of the recrystallised fraction by the statistical model (continuous line) and by hardness measurements (marks) in the 40% sample.

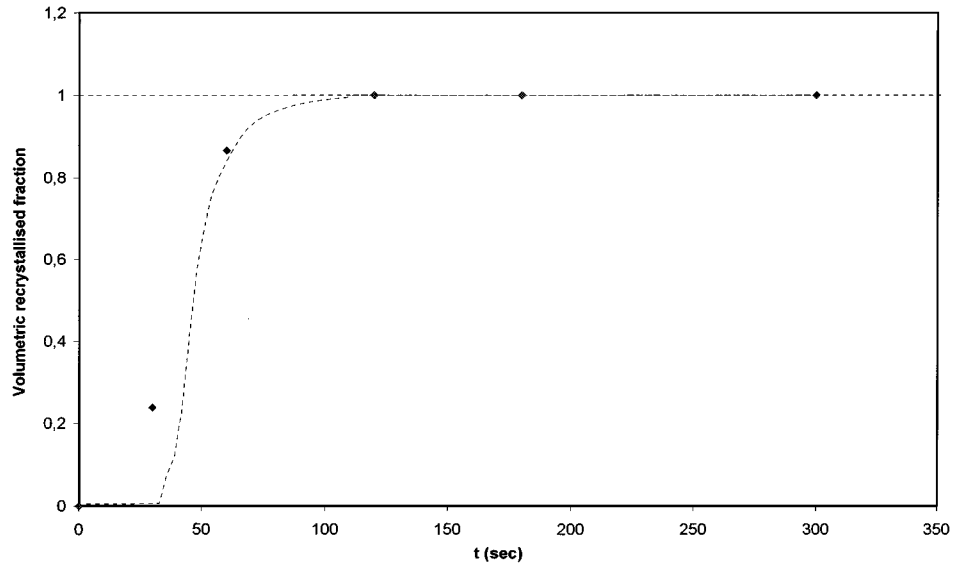

Figure 9 Comparison between the prediction of the recrystallised fraction by the statistical model (continuous line) and by hardness measurements (marks) in the 60% sample.

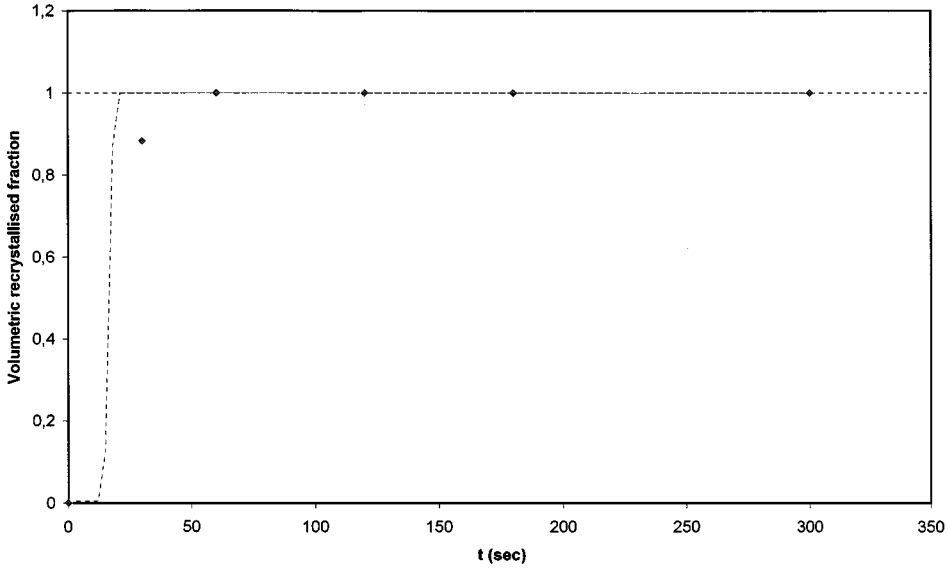

Figure 10 Comparison between the prediction of the recrystallised fraction by the statistical model (continuous line) and by hardness measurements (marks) in the 80% sample.

TABLE III Mean radius of samples with different reduction rates at times t_R corresponding to a complete recrystallization

Cold reduction grade, %	t_R (sec)	Mean radius (μm)
40	200	12.1
60	120	7.9
80	60	6.2

The good agreement obtained between indirect experimental data and model results confirms also in this case the good quality of the modelisation. In fact, the prediction of the evolution of the volume fraction by the recrystallization model (Figs 8–10) should be compared with experimental data (microstructure evolution) on volume fraction. However, at the present such measures are rather difficult to be performed with reasonable accuracy and reproducibility by metallographical methods because of the insufficient definition of the obtainable microstructure images. Then, Equation 15 provides a valid alternative to more direct experimental validation of the statistical model.

From the comparison between results reported in Figs 1–3 and Figs 8–10 it can be observed that at times corresponding to a complete recrystallization, the lower is the reduction rate the greater is the mean radius. This conclusion is in agreement with the fact that at higher cold reductions higher dislocation densities and thus higher numbers of nuclei are present in the steel with a consequent lower mean radius. These results are summarised in Table III.

5. Conclusions

Recrystallization and grain growth have been studied in samples of a low Ni steel subjected to different reduction grades. A mathematical model based on statistical assumptions has been developed and applied to predict the microstructural evolution of samples subjected to different heat treatments, taking into account the time dependence of the temperature in the expression of the mobility. An independent test on the quality of the fitting parameters has been performed, checking the correlation between the dislocation densities obtained by fitting the experimental data with the model and the mechanical properties obtained by tensile stress measurements.

Due to the general difficulty in measuring the recrystallized volume fraction F_V by automatic image analyser in partially annealed samples, a model has been developed correlating F_V to the hardness of the steel.

The results show a good agreement between experimental data and the prediction according to the statistical model.

References

1. A. I. BALITSKII, M. DIENER, R. MAGDOWSKI, V. I. POKHMURSKII and M. SPEIDEL, in Proceedings of the 5th International Conference on High Nitrogen Steels, Stockolm, July 1998, p. 401.
2. A. DI SCHINO, J. M. KENNY, M. G. MECOZZI and M. BARTERI, in Proceedings of the 20th Sampe International Conference, Paris, April 1999, edited by M. Erath, p. 175.
3. A. DI SCHINO, M. G. MECOZZI, M. BARTERI and J. M. KENNY, *J. Mater. Sci.* **35** (2000) 375.
4. *Idem., ibid.* **35** (2000) 4803.
5. G. STEIN, *Int. Jour. of Mat. and Product Tech.* **10** (1995) 290.
6. P. MARSHAL, "Austenitic Stainless Steels" (Elsevier Applied Science Publishers, 1984) Ch. 2, 27.
7. A. RECHSTEINER, in "Proceedings of the International Conference Innovation of Stainless Steels, Florence, October 1993, edited by AIM, p. 107.
8. K. W. MAHIN, K. HANSON and J. W. MORRRIS, *Acta Metall.* **28** (1980) 443.
9. T. O. SAETRE, O. HUNDERI and O. NES, *ibid.* **34** (1986) 981.
10. R. D. DOHERTY, A. R. ROLLETT and D. J. SROLOVITZ, in Proceedings of the 7th Int. Riso Symposium, Riso, 1986, edited by Hansen N.
11. M. HILLERT, *Acta Metall.* **13** (1965) 227.
12. J. W. CAHN and G. E. PEDAWAR, *ibid.* **13** (1965) 1091.
13. J. VON NEUMANN, "Metal Interfaces" (ASM, Cleveland, 1952) p. 108

14. K. LUCKE, R. BRANDT and G. ABBRUZZESE, *Mat. Science Forum* **19** (1996) 204.
15. G. ABBRUZZESE, *Acta Metall.* **33** (1985) 1329.
16. G. ABBRUZZESE and K. LUCKE, *ibid.* **34** (1986) 905.
17. *Idem., Mat. Science Forum* **55** (1996) 204.
18. I. SALVATORI and G. ABBRUZZESE, in 3rd International Conference on Grain Growth, Warrendale, June 1998, edited by TMS, p. 187.
19. DE HOFF and RHINES, "Quantitative Microscopy" (Mac Graw Hill Book Company, 1968).
20. W. JOST, "Diffusion" (Academic Press, New York, 1960) p. 239.
21. A. S. KEH and S. WEISSMAN, "Electron Microscopy and Strength of Crystals" (Interscience Publishers, 1963).

Received 6 December 1999
and accepted 13 July 2000